Radial Basis Function Networks Applied to QRST Cancellation in Atrial Fibrillation Recordings

J Mateo[1], A Torres[1], C Sánchez[1], JJ Rieta[2]

[1]Innovation in Bioengineering Research Group, Universidad de Castilla-La Mancha, Spain
[2]Biomedical Synergy, Electronic Engineering Dept., Universidad Politécnica de Valencia, Spain

Abstract

The analysis of the surface electrocardiogram (ECG) is the most extended noninvasive technique in medical diagnosis of atrial fibrillation (AF). In order to use the ECG as a tool for the analysis of AF, we need to separate the atrial activity (AA) from other cardioelectric signals. In this matter, statistical signal processing techniques, like independent component analysis (ICA) algorithms, are able to perform a multilead statistical analysis with the aim to obtain the AA. On the other hand time-domain-based techniques, like Average Beat Substraction (ABS), have been well accepted and used in clinical applications to cancel out the QRS complex and the T wave.

In this contribution, a QRST cancellation method based on a radial basis function (RBF) network is proposed. Average Results for the RBF method applied are (mean$\pm std$)Cros-Correlation=0.95± 0.021 *and* $MSE = 0.356 \pm 0.102$ *in contrast to traditional compared methods that, for the best case, yielded* $CC = 0.86 \pm 0.031$ *and* $MSE = 0.491 \pm 0.213$*. The results prove that RBF based methods are able to obtain a very accurate reduction of ventricular activity (VA), thus providing high quality atrial activity extraction in AF recordings.*

1. Introduction

Atrial fibrillation is a common arrhythmia with a prevalence of approximately 0.4-1.0% in the general population [1]. Prevalence increases with age and it is estimated to be present in 5% of those older than 65, and 10% of those older than 70 [2]. It is associated with an increased risk of stroke and mortality, as well as impaired exercise tolerance, fatigue, and heart failure [3, 4]. The diagnosis of AF, as such, has been based mainly on visual inspection of the surface electrocardiogram (ECG) [5]. Due to the much higher amplitude of the electrical ventricular activity (VA) on the surface ECG, cancellation of the ventricular involvement is crucial in the study of AF on ECGs. Two approaches are generally used to perform this task: source separation algorithms and matched template subtraction. Source separation algorithms try to find uncorrelated components using principal component analysis (PCA), or to find independent components in an instantaneous linear mixture using independent component analysis (ICA). PCA have previously been employed to monitor the effects of drugs [6] and assess the effects of linear left atrial ablation [7]. ICA has been applied in order to obtain ECG signals devoid of VA involvement [8, 9].

Other methods are based on standard or improved average beat subtraction (ABS) [10]. These methods assume that, in the same patient, ventricular complexes generally exhibit a limited number of forms. An average (template) of these distinct complexes is then used to subtract the VA. This method relies on the assumption that the average beat can represent approximately each individual beat. However, QRST morphology is often subject to minor changes caused by respiration, patient movement, etc, and, therefore, QRST residua and noise are often present in the estimated AA or remainder ECG [4].

In this paper, a QRST cancellation system, using a Radial Basis Function (RBF) network, is proposed. This RBF network has been developed like hierarchically layered structure. It starts with a small number of RBFs and then adds new RBFs if the approximation error is larger than some predetermined threshold and there is no existing RBF that can efficiently represent the current input. The adaptation strategy for the weight matrix of the RBF network is developed using the Lyapunov approach. Different types of RBFs can be employed by the proposed self-organizing RBF network. The implementations using Gaussian RBF (GRBF) are compared with PCA, ICA and ABS techniques.

2. Materials

In this study, two types of signals have been used. These have been referred to either real recordings from the PhysioNet Database [11] or synthetic signals.The sampling frequency used is $1kHz$. 100 recordings with different database (MIT-BIH Atrial Fibrillation Database, Long-Term AF Database, MIT-BIH Arrhythmia Database,

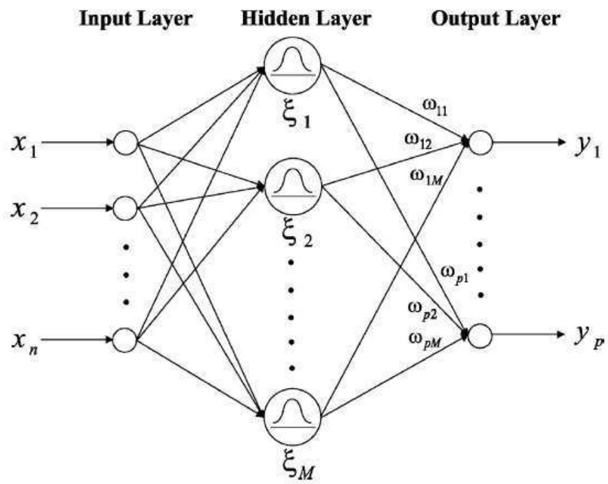

Figure 1. RBF neural network.

AF Termination Challenge Database...) have been selected from PhysioNet with different types of QRS morphologies and 100 synthetic signals with AA added [12]. The signal has been cut into three parts. The first was used for training, the second and the third was used to validate and compare the method.

3. Methods

The performance of an radial basis function neural network depends on the number and centers of the radial basis functions, their shapes, and the method used for learning the input–output mapping [13, 14]. One characteristic of these functions is that any function can be approximated by a linear combination of radial basis functions (i.e. $f(x) \approx \sum w_i \xi_j(x)$). Then, it's possible to do a linear combination of this type of data that approximates the function that generated these data. To achieve this approach, this study uses a regression where several radial basis functions have been used [15, 16, 17].

The proposed system in the present study consists of artificial neural network (ANN) with structure based on RBF [13, 14, 18]. This structure was initially made up of three layers: an input layer, one hidden layer made up of 30 neurons, and an output layer as shown in figure 1. It starts with a small number of RBFs and then adds new RBFs if the approximation error is larger than some predetermined threshold and there is no existing RBF that can efficiently represent the current input. The adaptation strategy for the weight matrix of the RBF network is developed using the Lyapunov approach [19].

In Fig. 1, we show the structure of the basic RBF network, which consists of one input layer, one output layer, and one hidden layer [20]. For the given input $x = [x_1 ... x_n]^T$, the overall response at the kth output neuron $1 \leq k \leq p$ has the form

$$y_k = \sum_{j=1}^{M} w_{kj} \xi_j \left(x; c_{(j)}, \sigma_{(j)}\right) = \tag{1}$$

$$= \sum_{j=1}^{M} w_{kj} \prod_{i=1}^{n} \phi \left(\frac{\left|x_i - c_{i(j)}\right|}{\sigma_{i(j)}} \right) \tag{2}$$

where w_{kj} is the weight from the jth hidden neuron to the jth output neuron. In the following, we use the notation $\xi_j(x) = \xi_j \left(x; c_{(j)}, \sigma_{(j)}\right)$, which refers to the RBF located at the jth hidden neuron. The vector $c_{(j)} = \left[c_{1(j)} ... c_{n(j)}\right]$ is the center of $\xi_j(x)$, and the parameter $\sigma_{i(j)}$, $i = 1, .., n$, is the radius or the width of $\xi_j(x)$ in the ith coordinate. Finally, $\phi : [0, \infty) \longrightarrow \mathbb{R}^+$ is the activation function, which characterizes the shape of the RBF, where $\mathbb{R}^+$ is the set of nonnegative real numbers. Usually, the activation function ϕ is constructed so that it is radially symmetric. The largest value of ϕ is obtained when $x_i = c_{i(j)}$, whereas the value of ϕ vanishes or becomes very small when $\left|x_i - c_{i(j)}\right|$ becomes large. Let $w_k = [w_{k1} ... w_{kM}]^T$ be the weight vector for the kth output neuron and let . We then rewrite the expression for the response of the kth output neuron as $y_k = w_k^T \xi(x)$, and the output vector of the RBF network can be represented as $y = W\xi(x)$, where $y = [y_1 ... y_p]^T$ and $W^T = [w_1 ... w_p]$ [13, 14, 18]. The GRBF is characterized by the following activation function [20]:

$$\phi \left(\frac{|x - c|}{\sigma} \right) = \exp \left(- \frac{(x - c)^2}{2\sigma^2} \right) \tag{3}$$

This network has been built by a hidden layer network. There have been created a number of candidate networks (H) which contains a number of hidden neurons in order to initiate the network learning. The value of H has been decided by means of a test. For each candidate network, the sum of absolute values of covariances have been calculated from Equation 4.

$$F_j = \frac{1}{N} \sum_{k=1}^{M-1} \left| \sum_{p=1}^{N} \left(y_{j,p} - \overline{y_j}\right) \left(e_{k,p} - \overline{e_k}\right) \right|, \quad j = 1, ..., H \tag{4}$$

where $y_{j,p}$ is the output of the jth candidate network for the pth training pattern. The parameter $\overline{y_j}$ is the mean of the jth hidden unit outputs, $e_{k,p}$ is the output error at the kth output unit for the pth training pattern and $\overline{e_k}$ is the mean of the output errors at the kth output unit. Then, the network with the maximum covariance F_j is selected as the most promisingly network to be initialized. An optimum value $H = 35$ has been obtained.

3.1. Performance assessment

The proposed method was thoroughly tested and compared with some of the previously published QRS cancellation techniques, using the quantitative measures of performance that will be next described. The QRS reduction was computed by comparing the estimated and the original ECG in terms of the cross-correlation (CC) and mean square error (MSE).

The performance of the studied methods was also tested on clinical data from Physionet. In these signals, the real AA on the ECG was obviously unknown. The performance was evaluated by estimating the ventricular depolarization reduction (VDR) [21], i.e., the beat-by-beat reduction of the R-peak amplitude that the algorithm under evaluation is able to achieve. Therefore, the VDR was a vector of values defined as:

$$VDR(dB) = 10 \log \left(R_{ECG} / R_{VR} \right) \tag{5}$$

where R_{ECG} is the R-peak amplitude of the original ECG, and R_{VR} is the residual R-peak amplitude of the atrial electrogram after ventricular activity reduction. Regarding the atrial segments, the performance was evaluated by measuring the waveform degree of similarity (S) [21]. Thereafter, similarity was a vector of values defined as

$$S = C_{ECG,VR} / \sigma_{ECG} \sigma_{VR} \tag{6}$$

where $C_{ECG,VR}$ is the covariance of the two atrial segments under evaluation (original and ventricular reduced), and σ_{ECG} and σ_{VR} are their standard deviations, respectively.

4. Results

In order to research the performance of different methods, which had been tested by means of the ECG recordings. As a guarantee for results, the whole procedure has been repeated all over ECG recordings.

Table 1 summarizes the obtained values of MSE, CC, VDR and S for ECG recording. Note that significant statistical differences between RBF and ABS-ICA are reported for all the studied parameters and the analyzed recordings.

As a graphical summary, figure 2 shows the estimated AA signals corresponding to a typical AF recording when ICA, ABS and RBF methods are applied. As can be appreciated, the estimated AA through RBF matches the original AA with more fidelity than ABS and ICA. This fact agrees with the CC index and the mse mean values presented in table 2. In addition, it can be observed that the AA extracted by ABS and ICA present QRS residua of larger amplitude, which is coherent with the calculated VDR mean value. This result justifies the higher similarity values obtained with RBF. In contrast, the AA obtained with ABS and ICA present notable sudden transitions.

Table 1. Results provided by the comparison between ICA, ABS and RBF obtained for simulated AF recordings. Values indicate mean ± standard deviation.

	ICA	ABS	RBF
CC	0.850±0.046	0.86±0.031	0.95±0.021
MSE	0.536±0.123	0.491±0.213	0.356±0.102
VDR	2.672±2.52	4.32±3.16	7.05±2.25
S(%)	0.886±0.022	0.915±0.034	0.994±0.002

Table 2. Results provided by the comparison between ICA, ABS and RBF obtained for clinical AF recordings. Values indicate mean ± standard deviation.

	ICA	ABS	RBF
VDR	2.128±2.31	4.23±3.02	7.01±2.23
S(%)	0.876±0.024	0.923±0.015	0.993±0.002

These methodologies were also applied to real ECGs. Because of the fact that the original AA was previously unknown, the CC coefficient and MSE could not be computed. As a consequence, only the VDR and S of atrial segments were computed. The obtained values of these parameters are presented in table 2. In the same way as with synthetic signals, the AA obtained with RBF presents lower ventricular residue and higher similarity between atrial segments than those obtained with ABS and ICA.

Finally, since RBF considers dynamics in the QRST waveform, a more accurate cancelation template is obtained. As a consequence, it behaves more robustly in those ECGs with variable QRST morphologies. In contrast, the AA estimated by ABS and ICA will be highly contaminated by QRST residua; see the figure 2.

5. Conclusions

This work has presented how the proposed RBF has been used to QRS-T cancellation from ECG recordings. Throughout all the stages, our RBF has been adapted by means of using the Lyapunov approach, which has been improved in order to achieve our target. By means of this improvement, RBF has obtained better values of CC, MSE values of CC. MSE, VDR and S than the other methods. The results have shown that RBF is able to obtain a very accurate representation of VA, thus providing high quality AA extraction in short and single-lead AF recordings. As a way of conclusion, suffice is to say that the neural network-based approach obtains both QRST reduction and low modification of AA results in comparison with systems which had been based on ICA and ABS methods.

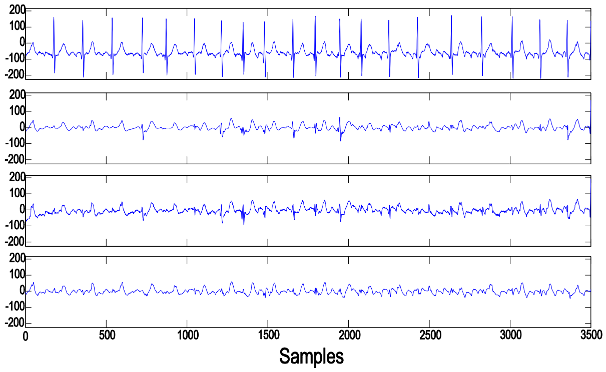

Figure 2. Comparison of QRST cancellation by RBF and standard filtering techniques of AF on ECGs. a) Original recording b) Results for ICA method. c) Results for ABS method d) Results for RBF method.

Acknowledgements

This work was partly sponsored by University of Castilla-La Mancha, TEC2010-20633 from the Ministry of Science and Education (Government of Spain), PII1C09-0036-3237, PII2C09-0224-5983 and the Patronato Universitario Cardenal Gil de Albornoz.

References

[1] Kannel W, Abbott R, Savage D, Mcnamara P. Epidemiologic features of chronic atrial-fibrillationŮ the framingham-study n. Engl J Med 1982;306:1018–1022.

[2] Fuster V, et al. Acc/aha/esc 2006 guidelines for the management of patients with atrial fibrillation: a report of the american college of cardiology. American Heart Association Task Force on practice guidelines and the European Society of Cardiology committee for practice guidelines developed in collaboration with th european heart rhythm association and the heart rhythm society Europace 2006; 8:651–745.

[3] Benjamin E, Wolf P, DŠAgostino R, Silbershatz H, Kannel W, Levy D. Impact of atrial fibrillation on the risk of death circulation 1998;946–952.

[4] Petrutiu S, Ng J, Nijm G, Al-Angari H, Swiryn S, Sahakian A. Atrial fibrillation and waveform characterization. a time domain perspective in the surface ecg. IEEE Eng Med Biol Mag 2006;25:24–30.

[5] Bollmann A, Husser D, Mainardi L, Lombardi F, Langley P, Murray A, Rieta JJ, Millet J, Olsson SB, Stridh M, Sörnmo L. Analysis of surface electrocardiograms in atrial fibrillation: techniques, research, and clinical applications. Europace 2006;8:911–926.

[6] Raine D, Langley P, Murrray A, Dunuwille A, Bourke JP. Surface atrial frequency analysis in patients with atrial fibrillation. J Cardiovasc Electrophysiol 2004;15:1021–1026.

[7] Raine D, Langley P, Murrray A, Furniss SS, Bourke JP. Surface atrial frequency analysis in patients with atrial fibrillation: Assessing the effects of linear left atrial abalation. J Cardiovasc Electrophysiol 2005;16:838–844.

[8] Vayá C, Rieta JJ, Sánchez C, Moratal D. Convolutive blind source separation algorithms applied to the electrocardiogram of atrial fibrillation: Study of performance. IEEE Trans Biomed Eng 2007;54(8):1530–1533.

[9] Rieta JJ, Castells F, Sánchez C, Zarzoso V, Millet J. Atrial activity extraction for atrial fibrillation analysis using blind source separation. IEEE Trans Biomed Eng 2004;51:1176–1186.

[10] Slocum J, Sahakian A, Swiryn S. Diagnosis of atrial fibrillation from surface electrocardiograms based on computer-detected atrial activity. J Electrocardiol 1992;25(1):1–8.

[11] Goldberger AL, Amaral LAN, Glass L, Hausdorff JM, Ivanov PC, Mark RG, Mietus JE, Moody GB, Peng CK, Stanley HE. PhysioBank, PhysioToolkit, and PhysioNet: Components of a new research resource for complex physiologic signals. Circulation 2000 (June 13);101(23):e215–e220. Circulation Electronic Pages: http://circ.ahajournals.org/ cgi/content/full/101/23/e215.

[12] Alcaraz R, Rieta JJ. Adaptive singular value cancelation of ventricular activity in single-lead atrial fibrillation electrocardiograms. Physiological Measurement 2008;29:1351–1369.

[13] Webb A, Shannon S. Shape-adaptive radial basis functions. IEEE Trans Neural Netw 1998;9(6):1155–1166.

[14] Lee CC, Chung PC, Tsai JR, Chang CI. Robust radial basis function neural networks. IEEE Trans Syst Man Cybern B Cybern 1999;29(6):674–685.

[15] Jianming L, Yonggon L, Sudhoff SD, Zak HSß. Self-organizing radial basis function network for real-time approximation of continuous-time dynamical systems. IEEE Trans Neural Netw 2008;19(3):460–474.

[16] Lin BS, Lin BS, Chong FC, Lai F. Higher-order-statistics-based radial basis function networks for signal enhancement. IEEE Trans Neural Netw 2007;18(3):823–832.

[17] Gonzalez J, Rojas I, Ortega J, Pomares H, Fernandez FJ, Diaz AF. Multiobjective evolutionary optimization of the size, shape, and position parameters of radial basis function networks for function approximation. IEEE Trans Neural Netw 2007;14(6):1478–1495.

[18] Karayiannis NB, Randolph-Gips MM. On the construction and training of reformulated radial basis function neural networks. IEEE Trans Neural Netw 2003;14(4):835–846.

[19] Angeli D. A lyapunov approach to incremental stability. IEEE Trans on Automatic Control 2002;47(3):410–421.

[20] Singla P, Subbarao K, Junkins JL. Direction-dependent learning approach for radial basis function networks. IEEE Trans Neural Netw 2007;18(1):203–222.

[21] Rieta JJ, Hornero F. Comparative study of methods for ventricular activity cancellation in atrial electrograms of atrial fibrillation. Physiological Measurement 2007; 28:925–936.